

Large-Solid-Angle Study of Pion Absorption on ^3He

T. Altholz,³ D. Androić,¹² G. Backenstoss,¹ D. Bosnar,¹² H. Breuer,⁵ A. Brković,¹² H. Döbbling,¹¹ T. Dooling,¹⁰ W. Fong,⁶ M. Furić,¹² P. A. M. Gram,⁴ N. K. Gregory,⁶ J. P. Haas,⁸ A. Hoffart,³ C. H. Q. Ingram,¹¹ A. Klein,¹⁰ K. Koch,¹¹ J. Köhler,¹ B. Kotlinski,¹¹ M. Kroedel,¹ G. Kyle,⁸ A. Lehmann,¹ Z. N. Lin,⁸ G. Mahl,¹¹ A. O. Mateos,⁶ K. Michaelian,¹¹ S. Mukhopadhyay,⁸ T. Petković,¹² R. P. Redwine,⁶ D. Rowntree,⁶ R. Schumacher,² U. Sennhauser,¹¹ N. Šimićević,⁶ F. D. Smit,⁷ G. van der Steenhoven,⁹ D. R. Tieger,⁶ R. Trezeciak,³ H. Ullrich,³ M. Wang,⁸ M. H. Wang,⁸ H. J. Weyer,^{1,11} M. Wildi,¹ and K. E. Wilson⁶

(LADS Collaboration)

¹University of Basel, CH-4056 Basel, Switzerland

²Carnegie-Mellon University, Pittsburgh, Pennsylvania 15213

³University of Karlsruhe, D-7500 Karlsruhe, Germany

⁴LAMPF, Los Alamos, New Mexico 87545

⁵University of Maryland, College Park, Maryland 20742

⁶Massachusetts Institute of Technology, Cambridge, Massachusetts 02139

⁷National Accelerator Center, Faure 7131, South Africa

⁸New Mexico State University, Las Cruces, New Mexico 88003

⁹NIKHEF-K, NL-1009 DB Amsterdam, The Netherlands

¹⁰Old Dominion University, Norfolk, Virginia 23529

¹¹Paul Scherrer Institute, CH-5232 Villigen PSI, Switzerland

¹²University of Zagreb, HR-41001 Zagreb, Croatia

(Received 6 April 1994)

Measurements have been made of π^+ absorption on ^3He at $T_{\pi^+} = 118, 162,$ and 239 MeV using the Large Acceptance Detector System. The nearly 4π solid angle coverage of this detector minimizes uncertainties associated with extrapolations over unmeasured regions of phase space. The total absorption cross section is reported. In addition, the total cross section is divided into components in which only two or all three nucleons play a significant role in the process. These are the first direct measurements of the total and three nucleon absorption cross sections.

PACS numbers: 25.80.Ls, 25.10.+s

Nuclear pion absorption at energies near that of the $\Delta(1232)$ resonance has been the focus of much attention in recent years [1–3]. The two-nucleon process, primarily absorption on $T = 0$ “deuteronlike” pairs, is experimentally well established and was initially expected to dominate the absorption process on all nuclei. However, more detailed studies have indicated that multinucleon mechanisms play a significant role. “Multinucleon mechanisms” refer to absorption processes that involve more than two nucleons, none of which acts simply as a spectator. It is sometimes appropriate to separate further those events which are characterized by signatures of known subprocesses, such as initial and final state interactions.

Indications of multinucleon absorption modes have been seen in discrepancies between the measured total absorption cross section and the measured two-nucleon absorption cross section on medium-heavy nuclei [4–8]. These modes are most easily studied in detail in ^3He and ^4He , where the effects of the addition of one or two nucleons to the absorbing system can be isolated.

Previous absorption experiments on these targets have shown the existence of multinucleon absorption modes [9–16]. However, they all suffered from some limitations in angular coverage or resolution, kinematic defini-

tion, or statistical precision for multiparticle final states. The Large Acceptance Detector System (LADS) was constructed at the Paul Scherrer Institute (PSI) to examine pion absorption reactions with an emphasis on multinucleon final states. LADS was designed to cover as much solid angle as possible with good energy and angular resolution. This Letter reports the total absorption cross section for π^+ absorption on ^3He at three energies around the Δ resonance. The partial cross sections for the cases in which only two or all three nucleons play a significant role in the absorption process are also reported.

The LADS detector (Fig. 1) [17] consists of a cylinder of 28 dE - E - E plastic scintillator sectors, each 1.6 m in active length and viewed by photomultiplier tubes at each end. The dE scintillators are 4.5 mm thick. The E layers can stop 200 MeV normally incident protons, with an energy resolution of 3% FWHM. The ends of the cylinder are closed by “end caps,” each consisting of 14 dE - E plastic scintillator sectors. More than 98% of 4π solid angle is covered by the scintillator.

For charged particles, trajectory information is provided by two concentric cylindrical multiwire proportional chambers (MWPCs). Combined, these give angular resolutions for charged particles of ~ 10 mrad FWHM.

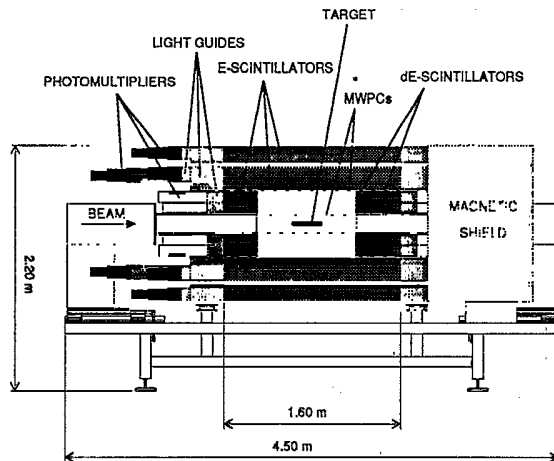


FIG. 1. A schematic representation of the LADS detector.

The target is a high pressure (95 bars) gas cylinder 25.7 cm in length with a 2 cm radius. Energy loss in the carbon fiber walls of the target and in the MWPCs dominates the threshold of the detector system, which is below 20 MeV for protons.

The data were collected in the $\pi M1$ area at PSI. The π^+ beam was defined using plastic scintillator detectors that counted individual pions. The defined beam rate was typically $10^5/s$ out of a total incident flux of about $3 \times 10^6/s$. Events were selected for analysis according to the number of charged and neutral particles detected in LADS in coincidence with a defined beam pion, and a fraction of each possible combination was written to tape.

There is only one significant final state for the absorption of a π^+ by ^3He : three unbound protons. Identification of the absorption reaction depends only on determining that there are no pions in the final state. The disappearance of the pion was determined by the requirement that more energy be deposited in the scintillators than the kinetic energy of the incident pion, assisted by energy vs dE/dx and energy vs time-of-flight particle identification techniques. The vertex of each event measured by the MWPCs was used to reject absorption events originating in the target's entrance and exit windows. Frequencies for the detection of two or of three protons from an absorption event were then determined.

It was necessary to correct these experimental frequencies for events lost due to reactions of the protons in the plastic scintillator (3%–18%); for wire chamber inefficiency (4%–10%); for background events (4%–15%); and for events in which scattered pions which reacted in the scintillator were classified as protons (0.2%–3.3%). The corrections vary with the incident pion energy over the range indicated and were all determined from the data. These corrections could be determined very accurately because it was always possible to select a representative set of absorption events using information independent from

the correction being determined. These events could then be passed through the normal analysis chain to determine the efficiency. The measurement of reaction losses is described in the next paragraph as an example.

To correct the yield for such losses when only two protons were detected, data were used from absorption on deuterium since the energy and angular distributions are similar to those from the two-nucleon absorption process on ^3He . Absorption events were selected from their angular correlations by the wire chambers, independently of the scintillator energy information. The fraction of these events lost while passing through the normal analysis chain determined the correction to the ^3He data. To correct the yield when three protons were detected a similar procedure was used, based on the angular correlation of protons from absorption on ^3He itself. There was a small amount of πpp contamination of the selected events in this case, the magnitude of which was determined from the spectrum of the total detected energy.

Several corrections had to be made to the measurement of the beam flux. The largest correction ($\leq 6\%$) was for pions missing the target and was determined by measuring the radial dependence of reactions in the air at both ends of the target. Other corrections were for beam impurity, pion decay, and attenuation due to nuclear reactions.

To obtain the total cross section, the data had to be corrected for the geometrical acceptance and energy threshold of the detector. For this correction a specific model of the absorption process was used to extrapolate over unmeasured regions. Prior experiments [9,14,15] have indicated that absorption on ^3He is apparently dominated by two distinct mechanisms: The first is two-nucleon quasifree absorption (2NA), in which the pion is absorbed on a deuteronlike pair inside the ^3He nucleus with a spectator proton. The second is a three-body mechanism (3NA), with a final state distribution similar to three-body phase space.

Monte Carlo simulations of these 2NA and 3NA processes were used to determine for each the fraction of the time LADS would detect two protons, and the fraction of the time it would detect three protons. The 2NA and 3NA cross sections were then determined from the experimental frequencies of these two possible results. The weighted average of the 2NA and 3NA corrections required for the total cross section were 15%, 13%, and 10% at 118, 162, and 239 MeV, respectively. Since these corrections are small, the determination of the total absorption on ^3He is not very sensitive to the details of the models.

The determination of partial cross sections for 2NA and 3NA is more dependent on the details of the simulations. Three-nucleon phase space was used to generate both the 2NA and the 3NA distributions. The former was weighted so that the spectator nucleon had a momentum distribution determined from theoretical

calculations of the ${}^3\text{He}$ ground state wave function [18]; these calculations are consistent with the results of quasifree ${}^3\text{He}(e, e'p)$ scattering [19,20]. It was also weighted so that the nucleons on which the absorption occurred had outgoing momenta and angular distributions consistent with Ritchie's parametrization [21] of absorption on deuterium. The specific characteristics of the detector were then taken into account in order to determine its response to each simulated event.

The assumption that absorption proceeds through the two above-mentioned mechanisms can be tested by comparing differential distributions measured by LADS with those produced by the simulations. Figure 2 shows the energy spectrum of the least energetic proton following an absorption reaction. When only two protons were detected, the energy of the third was reconstructed, with a cut on its reconstructed mass to select only ppp final states. Figure 2 also shows the results of the Monte Carlo simulations for 2NA and for 3NA, with magnitudes normalized to the data. The sum of the two Monte Carlos is plotted and reproduces the general features of the data, providing support for this model of the absorption process. Angular distributions have also been examined, and some interesting deviations from phase space in differential distributions for 3NA are indeed seen in the data. These will be addressed in a later publication; however,

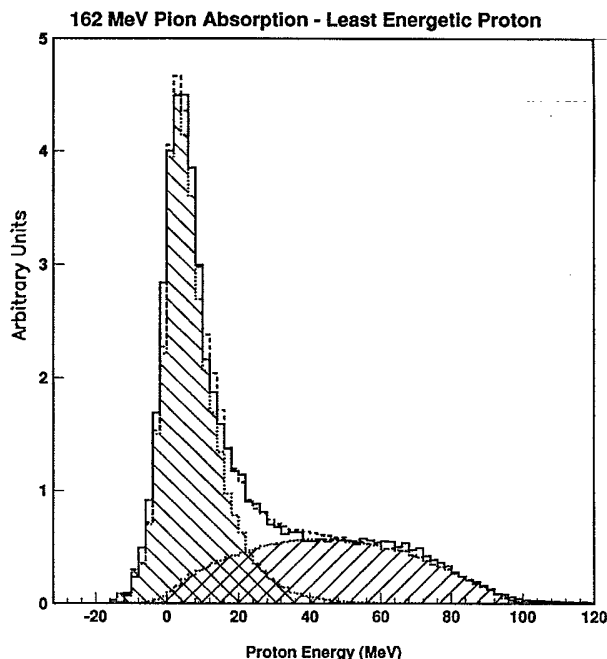


FIG. 2. The energy of the least energetic outgoing proton from the absorption of 162 MeV π^+ on ${}^3\text{He}$. The solid line is the data, the dotted lines are the results of the 2NA (the low energy peak) and the 3NA (the broad spectrum) simulations, and the dashed line is the sum of the two. The simulations include the effect of the detector's acceptance.

they are not significant for this measurement of integrated cross sections, which are determined directly by counting the number of absorption events with only small extrapolations over unmeasured phase space.

The cross sections are presented in Table I. Also included is the total cross section for absorption on deuterium measured by LADS, along with the values predicted by the parametrization of Ref. [21] for comparison. There were several experimental contributions to the systematic uncertainty of the total cross sections, with magnitudes up to 2.3%. These include uncertainties in the determination of the reaction losses, MWPC efficiency, acceptance, energy threshold, background subtraction, and normalization. No uncertainty was estimated for the assumption that absorption proceeds only through the 2NA and 3NA mechanisms, although uncertainties reflecting those in the final state angular distribution and in the initial state wave function of the absorbing pair were included. The latter includes the question of how the absorbing $T = 0$ pair differs from a real deuteron, and it dominates the uncertainty in the 3NA cross section.

Figure 3(a) shows the LADS results for the total absorption cross section on ${}^3\text{He}$ in comparison with previously reported data. Figure 3(b) is the same for the 2NA cross section, and Fig. 3(c) shows the 3NA cross section. At 118 MeV the cross sections are significantly larger than previously reported. It is important to note the agreement at this energy, as well as at the other two, between the measured cross section on deuterium and that from Ritchie's parametrization [21].

Because of the large acceptance of LADS, these results depend very little on assumptions about the angular distributions of the final state protons. This is especially important for 3NA as there are no prior experiments which investigate these distributions far from the reaction plane. The large coverage of the polar angle is also important for the measurement of 2NA since there are indications from both ${}^2\text{H}$ [21] and ${}^3\text{He}$ [13] that the second order Legendre polynomial typically used to extrapolate over unmeasured regions may not be adequate.

The ratio of 2NA on ${}^3\text{He}$ to absorption on ${}^2\text{H}$ has received considerable attention [2,3,23]. The LADS results for this ratio are 1.86 ± 0.10 , 1.60 ± 0.09 , and 1.63 ± 0.15 at 118, 162, and 239 MeV, respectively. The fact that this ratio is fairly close to 1.5 has sometimes been interpreted as an indication that the cross section scales simply with the number of $T = 0$ deuteronlike pairs in ${}^3\text{He}$. This, however, neglects possible effects in ${}^3\text{He}$ such as those due to the smaller internucleon spacing, the existence of more competing reaction channels, the larger binding energy, and initial and final state interactions.

In conclusion, cross sections have been measured for pion absorption on ${}^3\text{He}$. The total has been divided into 2NA and 3NA components, with 22%, 29%, and 30% of the total attributable to 3NA at 118, 162, and 239 MeV, respectively. These are the first results for the total and

TABLE I. Total cross sections for π^+ absorption on ^2H and ^3He . Also listed are the values of Ritchie's parametrization of absorption on ^2H [21], and the division into 2NA and 3NA components for the absorption on ^3He . Both systematic and statistical uncertainties are represented; the systematic uncertainties dominate.

T_{π^+} (MeV)	^2H		^3He		Total (mb)
	LADS (mb)	Ref. 21 (mb)	2NA (mb)	3NA (mb)	
118	11.5 ± 0.4	11.9	21.3 ± 1.0	6.0 ± 0.6	27.3 ± 0.8
162	10.9 ± 0.3	10.6	17.4 ± 0.8	7.2 ± 0.7	24.7 ± 0.7
239	4.3 ± 0.2	4.2	7.0 ± 0.6	3.0 ± 0.5	10.0 ± 0.4

three-nucleon absorption cross sections on ^3He coming from direct measurements without large extrapolations over unobserved regions, particularly regions out of the reaction plane. The significant 3NA cross section confirms previously reported results from detectors with much smaller solid angle coverage. However, the 2NA component and the total absorption cross section, while still roughly consistent with previous results, appear to peak at a lower energy than previously indicated. This

shift in peak energy brings observations on ^3He into better agreement with those on ^2H [21] and on ^4He [24,25].

We thank the staff of the Paul Scherrer Institute for their considerable assistance in mounting and running this experiment. This work was supported in part by the German Bundesministerium für Forschung und Technologie, the German Internationales Büro der Kernforschungsanlage Jülich, the Swiss National Science Foundation, the U.S. Department of Energy, and the U.S. National Science Foundation.

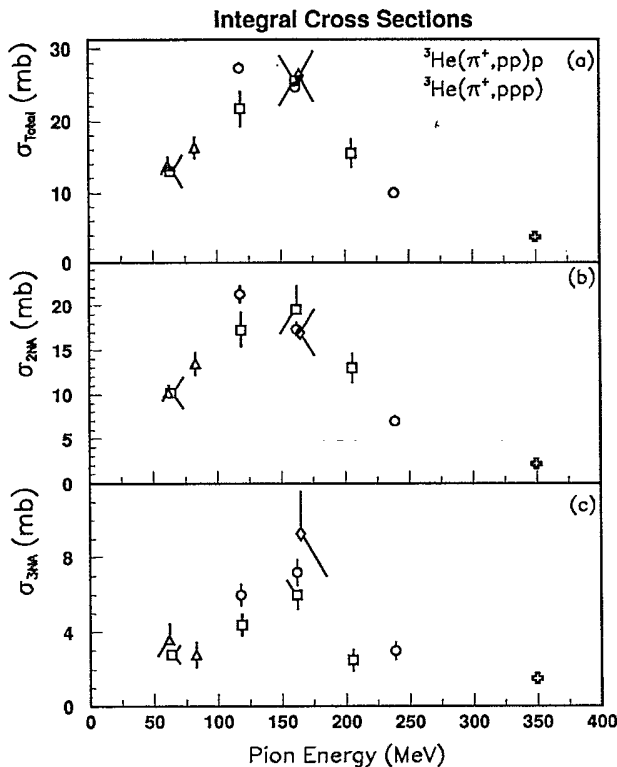


FIG. 3. The total absorption cross section (a) on ^3He as well as the 2NA (b) and 3NA (c) components, compared with previously published data. The circles are from this work, the triangles from Aniol *et al.* [22], the diamonds from Mukhopadhyay *et al.* [13], the crosses from Smith *et al.* [11], and the squares from Weber *et al.* [14].

- [1] D. Ashery and J.P. Schiffer, *Annu. Rev. Nucl. Part. Sci.* **36**, 207 (1986).
- [2] H.J. Weyer, *Phys. Rep.* **195**, 295 (1990).
- [3] C.H.Q. Ingram, *Nucl. Phys.* **A533**, 573c (1993).
- [4] D. Ashery *et al.*, *Phys. Rev. C* **23**, 2173 (1981).
- [5] A. Altman *et al.*, *Phys. Rev. Lett.* **50**, 1187 (1983); *Phys. Rev. C* **34**, 1757 (1986).
- [6] W.J. Burger *et al.*, *Phys. Rev. Lett.* **57**, 58 (1986); *Phys. Rev. C* **41**, 2215 (1990).
- [7] R.A. Schumacher *et al.*, *Phys. Rev. C* **38**, 2205 (1988).
- [8] S.D. Hyman *et al.*, *Phys. Rev. C* **47**, 1184 (1993).
- [9] G. Backenstoss *et al.*, *Phys. Rev. Lett.* **55**, 2782 (1985).
- [10] G. Backenstoss *et al.*, *Phys. Rev. Lett.* **61**, 923 (1988).
- [11] L.C. Smith *et al.*, *Phys. Rev. C* **40**, 1347 (1989).
- [12] M. Steinacher *et al.*, *Nucl. Phys.* **A517**, 413 (1990).
- [13] S. Mukhopadhyay *et al.*, *Phys. Rev. C* **43**, 957 (1991).
- [14] P. Weber *et al.*, *Nucl. Phys.* **A534**, 541 (1991).
- [15] P. Weber *et al.*, *Phys. Rev. C* **43**, 1553 (1991).
- [16] F. Adimi *et al.*, *Phys. Rev. C* **45**, 2589 (1992).
- [17] G. Backenstoss *et al.*, *Nucl. Instrum. Methods Phys. Res. A* **310**, 518 (1991).
- [18] Y. Wu, S. Ishikawa, and T. Sasakawa, *Few Body Systems* **15**, 145 (1993); S. Ishikawa and Y. Wu (private communication).
- [19] E. Jans *et al.*, *Phys. Rev. Lett.* **49**, 974 (1982).
- [20] C. Marchand *et al.*, *Phys. Rev. Lett.* **60**, 1703 (1988).
- [21] B.G. Ritchie, *Phys. Rev. C* **44**, 533 (1991).
- [22] K.A. Aniol *et al.*, *Phys. Rev. C* **33**, 1714 (1986).
- [23] K. Ohta, M. Thies, and T.-S.H. Lee, *Ann. Phys. (N.Y.)* **163**, 420 (1985).
- [24] Yu.A. Budagov *et al.*, *Sov. Phys. JETP* **15**, 824 (1962).
- [25] M. Baumgartner *et al.*, *Nucl. Phys.* **A399**, 451 (1983).